

## Partial melting and segregation behavior in a superplastic Si<sub>3</sub>N<sub>4</sub>/Al-Mg alloy composite

著者	Koike J., Mabuchi M., Higashi K.
journal or publication title	Journal of Materials Research
volume	10
number	1
page range	133-138
year	1995
URL	<a href="http://hdl.handle.net/10097/51943">http://hdl.handle.net/10097/51943</a>

doi: 10.1557/JMR.1995.0133

# Partial melting and segregation behavior in a superplastic Si<sub>3</sub>N<sub>4</sub>/Al–Mg alloy composite

J. Koike<sup>a)</sup>

Department of Mechanical Engineering, Oregon State University, Corvallis, Oregon 97331

M. Mabuchi

National Industrial Research Institute of Nagoya, 1 Hirate-cho, Kita-ku, Nagoya 462, Japan

K. Higashi

Department of Mechanical Systems Engineering, College of Engineering, University of Osaka Prefecture, Sakai, Osaka 593, Japan

(Received 18 January 1994; accepted 3 October 1994)

Al–Mg alloy (5052) composite reinforced with Si<sub>3</sub>N<sub>4</sub> particulates was investigated by transmission electron microscopy and electron energy loss spectroscopy. Partial melting was observed at matrix/reinforcement interfaces and matrix grain boundaries at a temperature near an optimum superplastic temperature. Segregation of solute elements (Mg and Si) was observed at the interfaces and grain boundaries. Both partial melting and solute segregation were found to depend on grain boundaries. The obtained results were explained by a decrease of the solidus temperature due to segregation whose extent depends on the type of the grain boundary structure.

## I. INTRODUCTION

Aluminum alloy matrix composites reinforced with SiC or Si<sub>3</sub>N<sub>4</sub> have been known to exhibit superplastic behavior at elevated temperatures. In many cases, superplasticity has been demonstrated at very high strain rates of more than  $10^{-2} \text{ s}^{-1}$ ,<sup>1-4</sup> far exceeding traditional values of less than  $10^{-4} \text{ s}^{-1}$ .<sup>5,6</sup> To date, previous efforts to understand the origin of the superplasticity at high strain rates have focused on the structure and chemistry (solute segregation) of interfaces between the aluminum matrix and reinforcements without paying much attention to grain boundaries of the matrix. One of the interesting observations is that the interfaces in an Al–Cu–Mg (2124) alloy reinforced with SiC are segregated with Cu and Mg.<sup>7</sup> The possibility has been suggested that the interfaces have a lower melting temperature than the interior of matrix grains and play an important role in superplastic deformation. However, typical aluminum composites have a substantial grain boundary area that is in the same order as the interface area. For example, in an Al–20 wt. % Si<sub>3</sub>N<sub>4</sub> particulate composite with an aluminum grain diameter of 1  $\mu\text{m}$  and a nitride particle diameter of 0.2  $\mu\text{m}$ , the area fraction of grain boundaries to interfaces is roughly estimated to be 1 : 2. Therefore, deformation mechanisms related to grain boundaries deserve careful consideration.

In fact, the presence of reinforcements and their interfaces with matrix grains are not a necessary condition for the superplasticity at high strain rates. The

superplasticity at high strain rates has been reported in various aluminum alloys without reinforcements.<sup>8</sup> It was found that the optimum strain rate for the superplasticity was independent of the type of the aluminum alloys and their processing method but dependent on the grain size. Preventing grain growth during superplastic deformation was shown to be an essential factor to realize the superplasticity at high strain rates. These results in the aluminum alloys and the composites suggest that microstructural characterization of general structural boundaries (both interfaces and grain boundaries) is essential in understanding the superplasticity mechanism.

Recently, we have performed *in situ* TEM observations and differential scanning calorimetry (DSC) at elevated temperatures to examine the possibility of partial melting in three types of aluminum alloy composites reinforced with Si<sub>3</sub>N<sub>4</sub> particulates.<sup>9</sup> The specimens were prepared in the same way as for the tensile specimens tested for the superplasticity in Refs. 2–4. It was found that a DSC scan showed a sharp endothermic peak at an optimum superplastic temperature of each composite. TEM observations at the same temperature revealed partial melting not only along the interfaces but also along the grain boundaries of the matrix alloys, suggesting easy sliding and/or migration of grain boundaries and interfaces during superplastic deformation. These results directly indicate the importance of partial melting in the superplasticity mechanism at high strain rates.

The present study has been aimed at understanding the origin of partial melting by investigating the segregation behavior along interfaces and grain boundaries. Analytical TEM was employed to examine the local chemical composition along interfaces and grain boundaries in the

<sup>a)</sup>Present address: Department of Materials Science, Faculty of Engineering, Tohoku University, Sendai 980, Japan.

aluminum-magnesium (5052) alloy composite reinforced with particulate  $\text{Si}_3\text{N}_4$ . Since segregation as well as mechanical properties has been known to depend on the structural type of grain boundaries, the dependence of segregation and melting on the grain boundaries and the interfaces was also investigated.

## II. EXPERIMENTAL PROCEDURE

A composite of an aluminum-magnesium (5052) alloy matrix reinforced with 20 wt. %  $\text{Si}_3\text{N}_4$  particulates was prepared by hot pressing of powder, followed by hot extrusion to form a billet. The chemical compositions of the matrix alloy are listed in Table I. A major alloying element is Mg with minor additions of Cr, Si, and Fe. This aluminum alloy composite exhibits the superplasticity at high strain rates under the conditions listed in Table II.<sup>3</sup> Notice that the optimum temperature was 818 K. An elongation of 700% could be achieved at a high strain rate of  $1 \text{ s}^{-1}$ . A TEM specimen was prepared by cutting a 3 mm disk from an as-extruded billet. The disk was thinned by mechanical grinding and ion milling to perforation for electron transparency. Ion milling was performed with 3-keV argon ions. During ion milling, the specimen was cooled to liquid nitrogen temperature in order to minimize irradiation damage.

The specimen was first heated to 821 K for *in situ* observation of melting at grain boundaries and interfaces. The specimen was then slowly cooled in the TEM to room temperature and removed from the specimen stage. In order to remove surface contamination, formed during *in situ* observation, the specimen was ion milled with a liquid nitrogen holder for 30 min. The segregation behavior was subsequently investigated by an electron energy loss spectrometer (EELS) attached to the TEM for microchemical analysis. An electron-beam diameter of  $\sim 2 \text{ nm}$  was obtained by using a field emission source. The actual beam size was expected to be slightly larger, particularly on the exit surface of the specimen because of scattering of electrons during interaction with the specimen. In order to minimize the multiple scattering

effects on inner-shell peaks, a very thin part of the specimen was analyzed by EELS. This also ensured that no other phases are overlapped in the analyzed area. Data acquisition time for each EELS spectrum was 10 s. During acquisition, both the specimen and the electron beam remained at the same position. It was considered that the chemical concentration was not altered noticeably before and after a heating-and-cooling cycle. This was supported by the experiment in a different specimen which showed a similar partial melting behavior at the same temperature during the first and second heating runs that were performed 24 h apart. Therefore, EELS analysis performed at room temperature could be utilized to discuss the effects of chemical composition on the microstructure observed at 821 K.

## III. RESULTS

Specimen temperature was increased stepwise by controlling an applied voltage to a heater, and the microstructural change was observed *in situ* by TEM. With increasing temperature from 816 to 821 K, a drastic change was observed in the microstructure as shown in Fig. 1. In the bright-field image in (a) taken at 821 K, rounded corners of the matrix grains (marked by arrows) appear, indicating the presence of the liquid phase. The diffraction pattern in (c) shows the diffuse ring intensity, superposed with a crystalline spot pattern. The diffuse ring pattern is indicative of the formation of the liquid phase. Polycrystalline rings, observed to overlap with a diffuse ring, are identified as surface contamination formed during observation and are, therefore, irrelevant to the intrinsic properties of the specimen. In a separate experiment with DSC, a sharp endothermic peak showed an onset at 821 K, confirming the melting reaction at this temperature. Since the onset temperature was determined by a crossing point of tangential lines of the DSC spectrum, some error may be included when this temperature is compared with other data.

TABLE I. Composition of the Al-Mg matrix alloy.

	Mg	Cr	Si	Fe	Cu	Mn	Ti	Zn	Al
Wt. %	2.46	0.25	0.16	0.16	0.04	<0.01	<0.01	<0.01	96.9
At. %	2.70	0.13	0.15	0.08	0.017	<0.005	<0.006	<0.004	96.9

TABLE II. Conditions for the superplasticity at high strain rates in  $\text{Si}_3\text{N}_4/\text{Al-Mg}$  alloy composite.

Elongation	Temperature	Strain rate sensitivity	Strain rate	Flow stress	Grain size	
					(Matrix)	( $\text{Si}_3\text{N}_4$ )
700%	818 K	0.3	$1 \text{ s}^{-1}$	6 MPa	$1 \mu\text{m}$	$0.2 \mu\text{m}$

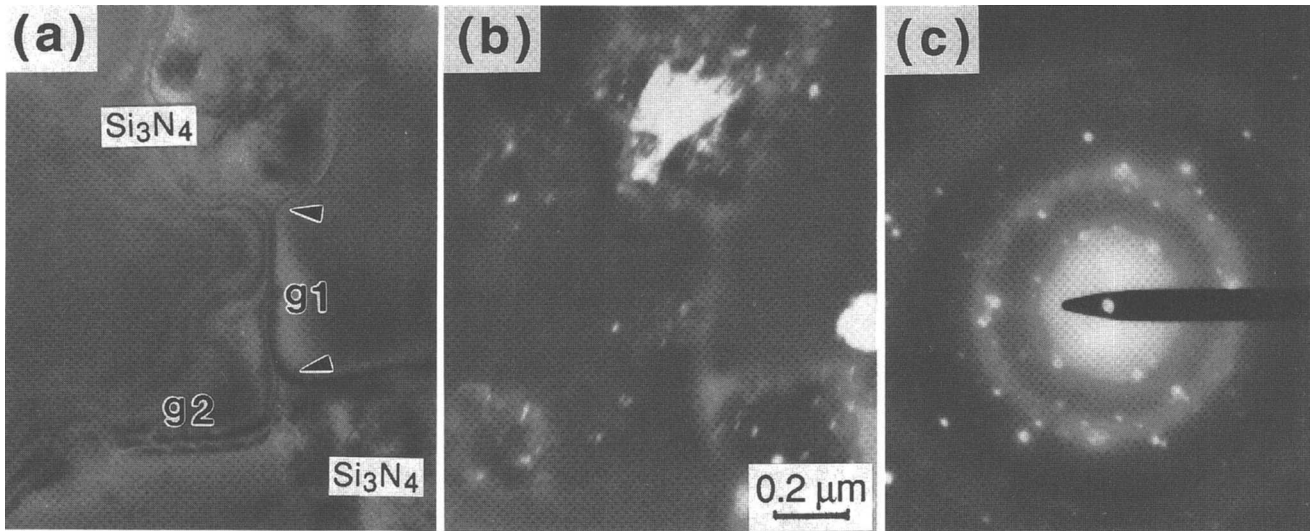


FIG. 1. (a) TEM bright-field and (b) dark-field images, and (c) selected area diffraction pattern of the Al-Mg composite at 821 K.

The observed shape change of grain corners depends on the relative magnitude of the energy ( $2\gamma_{ls}$ ) of the liquid-solid interface (or boundary) to the energy ( $\gamma_{ss}$ ) of the solid-solid interface (or boundary).<sup>10</sup> The liquid phase is localized only around triple junctions for  $2\gamma_{ls} > \gamma_{ss}$ , while the liquid phase exists throughout the interface (boundary) for  $2\gamma_{ls} < \gamma_{ss}$ . Moreover, sliding behavior is strongly influenced by the distribution of the liquid phase along the interfaces and boundaries. In order to clarify the liquid-phase distribution, a dark-field image is taken from a portion of the diffuse ring. As shown in Fig. 1(b), the bright intensity, indicating the presence of the liquid phase, is observed along the interface and one of the grain boundaries. Other brighter contrasts are a portion of  $\text{Si}_3\text{N}_4$  particles and surface contamination whose diffraction spots are inevitably included in the objective aperture for the dark-field imaging. It is thus concluded that the relation,  $2\gamma_{ls} < \gamma_{ss}$ , is satisfied in the Al-Mg composite and that the liquid phase exists along the grain boundary and interface.

It is emphasized that the tendency of melting appears to be dependent on grain boundaries, i.e., the type of grain boundary structure characterized by the misorientation between neighboring grains. In the bright-field image, two types of grain boundaries are observed and marked as g1 and g2. In the dark-field image, only the g1 grain boundary has a bright contrast, indicating melting. Quantitatively, the misorientation angle, determined from Kikuchi diffraction patterns, is  $18^\circ$  for the g1 boundary and  $3^\circ$  for the g2 boundary. The results suggest that the tendency of melting along the grain boundary is dependent on the misorientation angle between adjacent grains.

Segregation behavior is studied in connection with melting. Figure 2 shows an EELS spectrum taken by

a 2 nm electron probe centered at an arbitrarily chosen interface. The spectrum in (a) includes energy-loss peaks of magnesium at 1305 eV, aluminum at 1560 eV, and silicon at 1839 eV. It is revealed that magnesium atoms segregate along the interface. The magnesium segregation at matrix/reinforcement interfaces has been reported in other aluminum alloy composites reinforced with SiC.<sup>11,12</sup> The present result is consistent with these reports. The spectrum in (b) includes energy-loss peaks

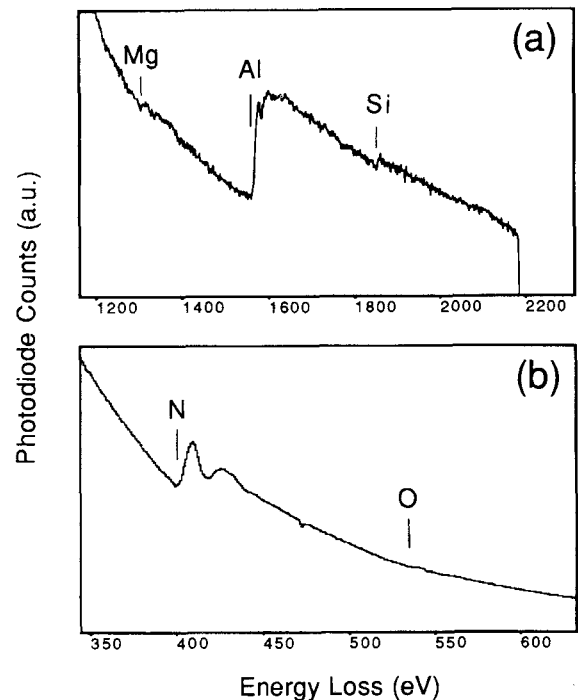


FIG. 2. Electron energy loss spectra from the interface region: (a) high energy loss region and (b) low energy loss region.

of nitrogen at 400 eV and oxygen at 532 eV, indicating the presence of oxygen at the interface in addition to nitrogen of  $\text{Si}_3\text{N}_4$ . The results of a grain boundary are shown in Fig. 3. It is found that the boundary is segregated with silicon, as shown in (a). However, the magnesium peak is absent at the boundary. Both nitrogen and oxygen are present, as shown in (b). It is noted that the vertical scale of this figure is expanded in comparison to Fig. 2(b) in order to better resolve the oxygen and nitrogen peaks. The concentration of each segregant is derived from the calculated single ionization cross section and the experimentally obtained peak area after background subtraction.<sup>13</sup> Table III summarizes the atomic ratios of segregants to aluminum. The extent of segregation is also qualitatively investigated at several interfaces and grain boundaries. Preliminary results indicate that segregation occurs at most interfaces (6 segregated interfaces out of 7 investigated) and the extent is nearly independent of the interfaces. On the other hand, segregation is observed at only two of the seven grain boundaries investigated (1 strongly segregated and 1 weakly segregated). This grain-boundary dependent segregation is consistent with the reports in various alloys.<sup>14-16</sup>

#### IV. DISCUSSION

The solute concentrations measured in the present work may be lower than the true concentration at the interfaces and boundaries because of the possibility

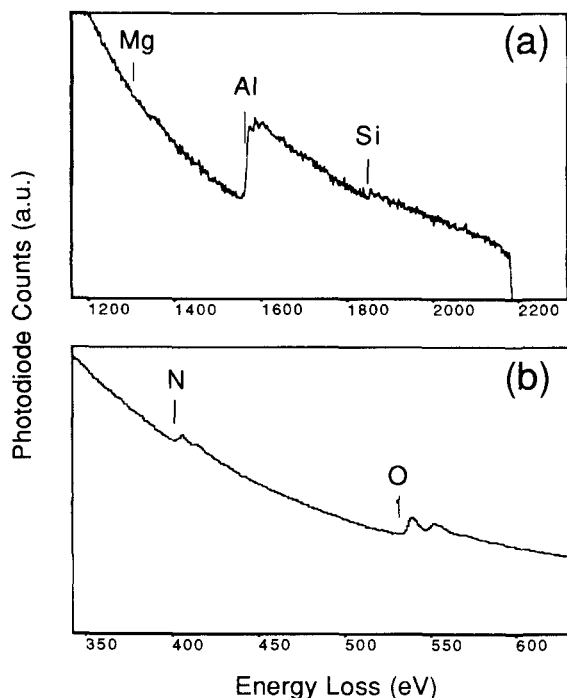


FIG. 3. Electron energy loss spectrum from the grain boundary region: (a) high energy loss region and (b) low energy loss region.

of the electron beam diameter being larger than the width of the segregation profile. Strangwood *et al.*<sup>7</sup> have studied the segregation profile in various aluminum alloy composites reinforced with SiC by using a 2 nm electron beam. With increasing annealing time, they found that the width of the segregation profile of solute atoms (Mg, Cu, and Zn) decreased from 20–50 nm to 2.5–5 nm, which was comparable to the beam diameter. When Auger electron spectroscopy was used in conjunction with ion sputtering,<sup>17</sup> the concentration of segregants was found to drop rapidly within a grain-boundary layer of 1–2 nm in width. Therefore, the concentration of segregants measured in the present work, as well as by Strangwood *et al.*,<sup>7</sup> seems to be an averaged value over the probed area of 2 nm diameter as if a constant concentration is assumed. The true concentration at the grain boundary and at the interface can be much larger than the measured concentrations if the observed segregation results from an equilibrium condition.

L'Espérance *et al.*<sup>12</sup> and Nieh and Wadsworth<sup>18</sup> have proposed that the solute segregation can lower the melting point of segregated layers. According to the binary phase diagrams of Al–Mg<sup>19</sup> and Al–Si,<sup>20</sup> magnesium addition to the pure aluminum up to 18.6 at. % lowers the melting point by 11 K per 1 at. % Mg. Beyond 18.6 at. %, the alloy melts at 723 K. Similarly, silicon addition to pure aluminum up to 1.5 at. % lowers the melting point by 56 K per 1 at. % Si. Beyond 1.5 at. %, the alloy melts at 850 K. Therefore, if the interface is segregated with more than 18.6 at. % of magnesium, the interface can melt at a eutectic temperature of 723 K. In fact, DSC results<sup>9</sup> showed that a weak endothermic reaction was initiated at 730–750 K and continued until a major endothermic reaction occurred at 821 K. The striking similarity between the eutectic temperature of Al–Mg alloys and the onset temperature of the endothermic reaction suggests that some interfaces are so enriched with magnesium that they can melt at a temperature as low as 723 K. Variation in magnesium and silicon concentrations is expected to change the melting point at different boundaries and interfaces. This may be a reason for a continuous endothermic reaction at higher temperatures. One may argue that the presence of oxygen and nitrogen can consume segregating magnesium and silicon by forming

TABLE III. Concentration of segregants in at. % at the interface and grain boundary.

	Mg	Si	N	O
Interface	9.3	<sup>a</sup>	<sup>a</sup>	3.2
Grain boundary	<sup>b</sup>	2.5	1.0	3.9

<sup>a</sup>Strong peaks from a  $\text{Si}_3\text{N}_4$  particle are detected.

<sup>b</sup>The peak is not detected in all seven grain boundaries.

various ceramic compounds as well as intermetallic compounds.<sup>7,11,12,21-23</sup> However, these compounds are all very stable and do not melt in the temperature range where the experiment was conducted. Therefore, we believe that a substantial amount of magnesium and silicon remains isolated without forming the compounds and contributes to lower the melting temperature at the interfaces and grain boundaries.

The present work has revealed that the tendency of melting depends on grain boundaries. This can be understood by the grain-boundary dependent segregation, characterized by the misorientation angle between neighboring grains. Watanabe and his co-workers have systematically studied the extent of segregation as a function of misorientation angle in Fe(Si)<sup>14</sup> and Fe(Sn).<sup>15</sup> They found that the extent of segregation increased with increasing the tilting angle except for low energy special boundaries. Similar observations have been reported in Cu(Bi) by Fraczkiewicz and Biscondi.<sup>16</sup> These observations support our view of partial melting that is caused by segregation whose extent depends on the grain boundary structure. On the other hand, the tendency of melting appears to be independent of the interface types. This may be caused by a strong chemical interaction of magnesium atoms with Si<sub>3</sub>N<sub>4</sub> particles. It would be interesting to study further the quantitative correlation among the grain-boundary structure type, the segregant concentration, and the tendency of melting.

It now appears that the role of reinforcement particles to the superplasticity are only to prevent grain growth. Since segregation can take place at the grain boundary without reinforcements, it should be possible to demonstrate the superplasticity at high strain rates in the matrix alloys by themselves. In fact, it has been recently reported that some alloys without any reinforcements exhibit superplasticity at testing temperatures very near or above their solidus temperatures.<sup>24-26</sup> However, one should bear in mind that even if the liquid phase exists along the boundaries, the superplasticity appears only when certain conditions are met. Such conditions may include thermal, microstructural, and mechanical conditions. For example, the liquid boundary can cause premature failure by forming cavities and microcracks under tensile stress conditions.<sup>27</sup> There are many cases in which the liquid phase causes brittle fracture<sup>28</sup> or premature creep failure.<sup>29</sup> The state of the liquid phase and the way it contributes to the deformation process are influenced by various experimental conditions and, thus, are important subjects to be explored further.

## V. SUMMARY

The formation of liquid phase was observed along the interface and grain boundaries. Segregation of Si at the grain boundaries and Mg at the interfaces was

identified and proposed to be a key reason for partial melting. The tendency of melting was found to depend on the grain boundaries, probably because of the observed dependence of segregation on the grain boundary structure. Some interface and boundaries may be so strongly segregated that partial melting may occur at a temperature as low as 723 K.

## ACKNOWLEDGMENTS

High temperature *in situ* observations were performed at the Center for Materials Science, Los Alamos National Laboratory with generous permission by Dr. T. E. Mitchell. Chemical analysis was performed at the Center for High Resolution Electron Microscopy, which is supported by NSF under Grant No. DMR-9115680. Technical support by the CHREM staff is greatly appreciated.

## REFERENCES

1. T. G. Nieh, C. A. Henshall, and J. Wadsworth, *Scripta Metall.* **18**, 1405 (1984).
2. M. Mabuchi, K. Higashi, Y. Okada, S. Tanimura, T. Imai, and K. Kubo, *Scripta Metall. et Mater.* **25**, 2003 (1991).
3. M. Mabuchi, K. Higashi, K. Inoue, and S. Tanimura, *Scripta Metall. et Mater.* **26**, 1839 (1992).
4. M. Mabuchi, K. Higashi, S. Wada, and S. Tanimura, *Scripta Metall. et Mater.* **26**, 1269 (1992).
5. C. H. Hamilton, C. C. Bampton, and N. E. Paton, *Superplastic Forming of Structural Alloys*, edited by N. E. Paton and C. H. Hamilton (TMS AIME, Warrendale, PA, 1982), p. 173.
6. C. C. Bampton, J. A. Wert, and M. W. Mahoney, *Metall. Trans.* **13A**, 193 (1982).
7. M. Strangwood, C. A. Hipsley, and J. J. Lewandowski, *Scripta Metall. et Mater.* **24**, 1483 (1990).
8. K. Higashi, *Mater. Sci. Eng.* **A166**, 109 (1993).
9. J. Koike, M. Mabuchi, and K. Higashi, *Acta Metall. et Mater.* (to be published).
10. D. R. Clarke and M. L. Gee, *Materials Interfaces*, edited by D. Wolf and S. Yip (Chapman and Hall, New York, 1992), p. 255.
11. S. R. Nutt and R. W. Carpenter, *Mater. Sci. Eng.* **75**, 169 (1985).
12. G. L'Espérance, T. Imai, and B. Hong, *Superplasticity in Advanced Materials*, edited by S. Hori, M. Tokizane, and N. Furushiro (The Japan Society for Research on Superplasticity, Osaka, Japan, 1991), p. 379.
13. R. F. Edgerton, *Electron Energy Loss Spectroscopy in the Electron Microscope* (Plenum Press, New York, 1986), p. 262.
14. T. Watanabe, S. Kitamura, and S. Karashima, *Acta Metall.* **28**, 455 (1980).
15. T. Watanabe, T. Murakami, and S. Karashima, *Scripta Metall.* **12**, 361 (1978).
16. A. Fraczkiewicz and M. Biscondi, *J. Phys.* **C4**, 497 (1985).
17. H. L. Marcus, L. H. Hackett, Jr., and P. W. Palmberg, *ASTM Data Series*, STP 499 (1972), p. 90.
18. T. G. Nieh and J. Wadsworth, *JOM* **11**, 46 (1992).
19. J. L. Murray, *Bull. Alloy Phase Diagrams* **3**, 60 (1982).
20. J. L. Murray and A. J. McAlister, *Bull. Alloy Phase Diagrams* **5**, 74 (1984).
21. X. G. Ning, J. Pan, K. Y. Hu, and H. Q. Ye, *Philos. Mag. A* **66**, 811 (1992).
22. H. Ribes, M. Suery, G. L'Espérance, and J. G. Legoux, *Metall. Trans.* **21A**, 2489 (1990).

23. N. Wang, Z. Wang, and G. Weatherly, *Metall. Trans.* **23A**, 1423 (1991).
24. N. Furushiro and S. Hori, in *Superplasticity in Metals, Ceramics, and Intermetallics*, edited by M.J. Mayo, M. Kobayashi, and J. Wadsworth (Mater. Res. Soc. Symp. Proc. **196**, Pittsburgh, PA, 1990), p. 249.
25. K. Higashi, S. Tanimura, and T. Ito, in *Superplasticity in Metals, Ceramics, and Intermetallics*, edited by M.J. Mayo, M. Kobayashi, and J. Wadsworth (Mater.
26. K. Higashi, T. Okada, T. Mukai, and S. Tanimura, *Scripta Metall. et Mater.* **25**, 2053 (1991).
27. J-G. Wang and R. Raj, *J. Am. Ceram. Soc.* **67**, 385 (1984).
28. M. C. Roth, G. C. Weatherly, and W. A. Miller, *Acta Metall.* **28**, 841 (1980).
29. G. M. Pharr, P. S. Godavarti, and B. L. Vaandrager, *J. Mater. Sci.* **24**, 784 (1989).